MEMS ABOVE CMOS PROCESS FOR SINGLE PROOF-MASS 3-AXIS LORENTZ-FORCE RESONANT MAGNETIC SENSOR

W. L. Sung[1], F. Y. Lee[1], C. L. Cheng[1], C. I Chang[2], E. Cheng[1, 3] and W. Fang[1, 2]
[1]Power Mechanical Engineering Department, [2]Institute of NanoEngineering and MicroSystems
National Tsing-Hua University, Hsinchu, Taiwan
[3]Taiwan Semiconductor Manufacturing Company Ltd., Hsinchu, Taiwan

ABSTRACT

This study designs and implements a silicon-based 3-axis Lorentz-force resonant magnetic sensor with single proof-mass using TSMC bulk MEMS above standard CMOS process [1]. The device is a 3-axis resonant-type sensor driven by single current loop. When the magnetic fields applied, the Lorentz-force is induced by current-carrying spring-mass structure and driven the structure at resonant frequency. Capacitance sensing electrodes could detect the dynamic responses of spring-mass system to determine the intensity of magnetic fields. Features of this study: (1) novel spring design acts as current-carrying and enables torsional/in-plane translational motions by magnetic fields; (2) single proof-mass and current loop for 3-axis magnetic fields detection; (3) fully compatible with MEMS inertial sensors process platform. A 1mm×1mm single proof-mass structure with gap-closing sensing electrodes for 3-axis magnetic fields detection is demonstrated.

INTRODUCTION

Magnetic sensors have been widely used in consumer products, like electronic compasses and location-based navigation applications. In these applications, the existing dominant technologies of magnetic sensors are utilizing the Hall effect [2-3] and Magnetoresistive (MR) effect [4]. The Hall effect magnetic sensors is compatible with standard CMOS process, but have lower sensitivity. On the other hand, the MR magnetic sensors have a higher sensitivity, but the hysteresis and requiring specialized magnetic materials are two concerns.

To overcome these challenges, the Lorentz-force magnetic sensors with MEMS structures have been extensively investigated [5-10]. The Lorentz-force, which is induced by the input current and magnetic field, can deform the suspended MEMS structures. Thus, the deformation of MEMS structures can be exploited to measure the magnetic fields. Moreover, when the input AC current is at the resonant frequency of the MEMS structure, deformed motion can be amplified by the mechanical quality factor. Typically, the resonant-type magnetic sensor has the advantage of high resolution, low power consumption, and without magnetic materials [5-6]. Furthermore, the resonant-type magnetic sensor could be monolithically integrated with other inertial sensors (i.e. gyroscopes and accelerometers) for inertial measurement unit (IMU) applications. Generally, for Lorentz-force magnetic sensors, the in-plane (X/Y-axis) magnetic field will introduce an out-of-plane motion, and the out-of-plane (Z-axis) magnetic field will introduce an in-plane motion of the MEMS structure. Thus, it's not straightforward to detect the 3-axis magnetic field simultaneously by a single MEMS structure. Most of the Lorentz-force magnetic sensors can only detect single-axis [7-8] or two-axis [6, 9] magnetic fields by a single proof-mass structure. There are few literatures presenting the single proof-mass 3-axis magnetic sensors utilizing the different sensing mechanism [5] and different input current loops [10].

This study presents a single proof-mass, Lorentz-force resonant magnetic sensor, which is capable of sensing 3-axis magnetic field and reduce the sensor footprint. A single current loop is designed in this study to introduce the Lorentz-forces for 3-axis magnetic fields detection. Moreover, due to the springs and structural design, this magnetic sensor can precisely identify the direction of the magnetic fields using both the torsional/in-plane translational motions. Furthermore, this device is realized by the TSMC MEMS above CMOS process [1]. This process scheme leverages the monolithic integration of suspended MEMS structures and CMOS substrate. Moreover, the future integration of magnetic sensor with other inertial sensors can also be achieved using the process scheme.

DESIGN CONCEPT

Fig. 1 illustrates the schematic design of the proposed 3-axis Lorentz-force resonant magnetic sensor. The

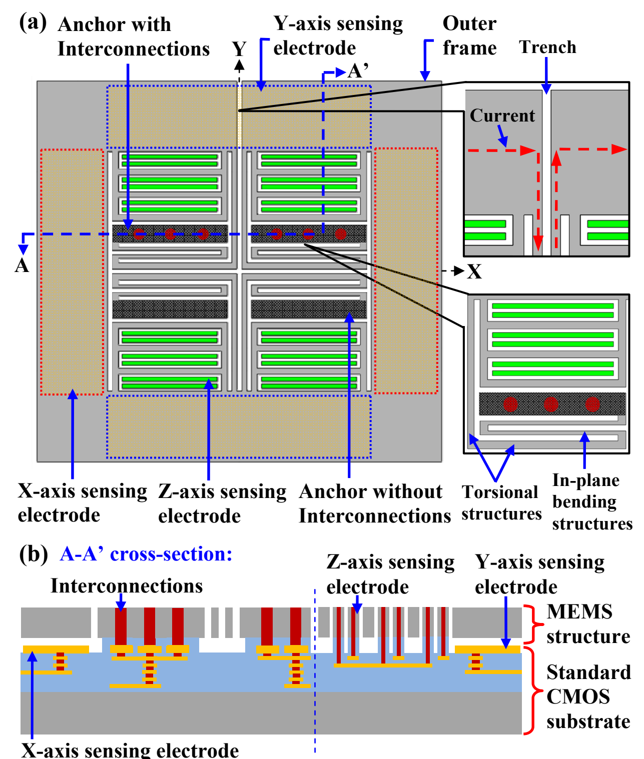

Figure 1: Schematic of 3-axis resonant magnetic sensor, (a) design concept of magnetic sensor and zoom-in configuration, and (b) graph of A-A' cross-section.

magnetic sensor consists of single proof-mass (outer-frame), connection springs, and sensing electrodes, as shown in Fig.1a. Four anchors are located near the center of sensor, and only two anchors have the electrical interconnections between CMOS and MEMS layers (i.e. for current input and output). The outer-frame is designed to sense the out-of-plane Lorentz-force (by see-saw motion) through the gap-closing sensing w.r.t the bottom X-axis and Y-axis electrodes. On the other hand, the in-plane Lorentz-force can be picked-up by the gap-closing sensing w.r.t. the Z-axis electrodes. As shown in the lower zoom-in graph in Fig.1a, this study presents a novel spring design which consists of the in-plane bending structures (for Z-axis magnetic field) and out-of-plane torsional structures (for X-axis and Y-axis magnetic field). Moreover, due to the trench design of the outer frame (as shown in the upper zoom-in graph in Fig.1a), a single current loop is restricted on the MEMS structure. Thus, such design enables the sensing of 3-axis magnetic fields through the Lorentz force excitations without the requirement of changing the current path. Fig.1b shows the graph of A-A' cross-section. The thick silicon layer (30μm) is employed as MEMS structures and stacked directly on the CMOS substrate with electrical routings. The interconnections serve as the electrical connection between the CMOS and MEMS layers, thus, can pass through the input and output currents.

Fig.2 shows the principles for 3-axis magnetic fields sensing. In Fig.2a, the current flow begins at one anchor (with interconnections) and, due to the trench design, passes through the spring and outer frame in the clockwise (or counter clockwise) direction. This single current loop results in the asymmetric current path on the outer frame, thus, is suitable for in-plan magnetic field sensing. For example, as the X-axis magnetic field exerted on the device (Fig.2b), the Lorentz-forces introduced by the current flow (solid red lines) will generate a torque along the Y-axis. Note that the current flow, which is paralleled to the direction of the magnetic field (as shown in dashed white lines), will not generate Lorentz-force. Moreover, due to small distance to the torsional axis, the torque induced by the current flow on the connection springs (dashed red lines) can be ignored. The Y-axis magnetic field sensing is similar to X-axis (as shown in Fig.2c), which is contributed to the single current loop design. Furthermore, for the Z-axis magnetic field sensing (Fig.2d), the Lorentz-forces generated by the current flows on the outer frame will cancel each other (dashed red lines). Thus, the Lorentz-forces are eliminated except those on x-axis torsional springs (solid red line). The net force will cause an in-plane linear motion along Y-axis. Finally, the above torsional/in-plane translational motions will be detected by the gap-closing sensing w.r.t. the X-, Y- and Z-axis electrodes. Fig.3 indicates the modal simulations of the magnetic sensor. The sensing modes are respectively 2.76kHz (Y-axis), 6.67kHz (Z-axis), and 7.37kHz (X-axis).

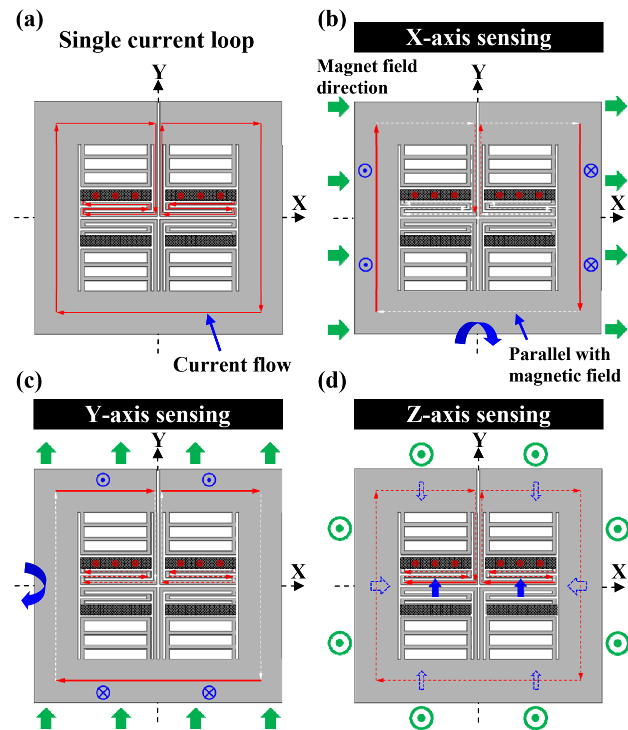

Figure 2: Sensing mechanism of 3-axis magnetic field, (a) input current loop, and (b-d) X/Y/Z-axis sensing mechanism.

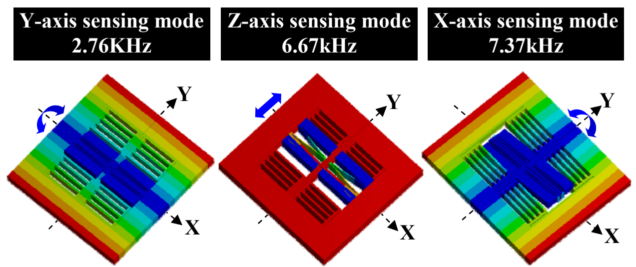

Figure 3: Simulation results of 3-axis resonant frequencies.

FABRICATION AND RESULTS

This device is realized using TSMC MEMS above CMOS platform, which is established for sensors

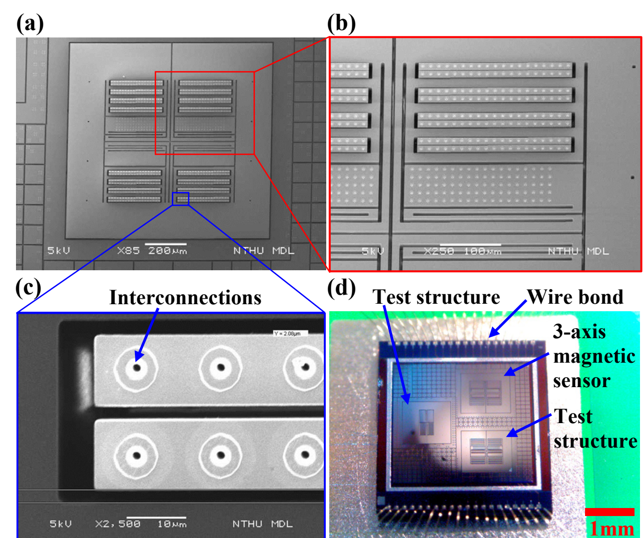

Figure 4: Fabrication results, (a-c) SEM photographs of 3-axis magnetic sensor, and (d) magnetic sensor chip after wire bonding.

implementation and integration [1, 11] (as shown in Fig.1b). In this process scheme, the thick single crystal silicon as the MEMS structure layer is stacked on top of a standard TSMC 0.18μm 1P6M CMOS substrate. The CMOS substrate offers the sensing electrodes and electrical routing for MEMS devices.

Fig.4 shows a typical fabricated sensor chip. Fig.4a shows the SEM micrograph of the whole magnetic sensor. The footprint of the magnetic sensor is about 1mm × 1mm. The SEM micrograph in Fig.4b indicates the zoom-in view of connection spring design, including the in-plane bending structure and out-of-plane torsional structures. Fig.4c shows the zoom-in view of z-axis sensing electrodes. The interconnections can be clearly observed, and the gap of the in-plane sensing electrodes is 2μm. Fig.4d shows the sensor chip after wire-bonded on PCB for testing purpose. The total chip size is 3.5mm × 4mm, including the 3-axis magnetic sensor and the testing structures.

MEASUREMENT

Measurement results shown in Fig.5 indicate the resonant frequencies of the 3-axis magnetic sensor. It accomplished by the commercial readout circuit (MS3110) and recorded by the network analyzer. The measurement results indicate the Y-axis sensing mode is at 2.27 kHz with Q~27.6, Z-axis sensing mode is at 5.83 kHz with Q~1479.4, and X-axis sensing mode is at 6.58 kHz with Q~156.2. The measured resonances are 11%~18% smaller compared to the simulation results (as in Fig.3) due to the dimension variation of structures caused by process.

Fig.6 shows the characterizations of the 3-axis magnetic sensor. Fig.6a shows the setup of magnetic field measurement. The test chip is placed inside the vacuum chamber (pressure is ~20torr) for air damping reduction. The input magnetic field is generated by the Helmholtz coil, and calibrated by a commercial gauss meter. The location of the magnetic sensor is well controlled at the center of the Helmholtz coil utilizing a positioning stage. An input signal, with DC offset 1.5V and AC amplitude 0.5V at the resonances, is applied to the MEMS structure, implying the corresponding input current of 4.3 mA. To distinguish the sensing signals and avoid feedthrough signals at the resonances [9], a 5-Hz sinusoidal current is applied to the Helmholtz coil to generate a low frequency magnetic field. As the device starts vibrating by the exerted Lorentz-force, a motional current is generated through the capacitive sensing electrodes. This current can be picked up by an active probe (gain=0dB), and the readout signals are recorded by the spectrum analyzer. The measured output spectra in response to the X-axis magnetic field (5-Hz, with the intensity of 50μT and 100μT) are shown in Fig.6b and Fig.6c respectively. The central tones indicate the feedthrough due to the AC input signal at the resonant frequency, and the sidebands indicate the sensing signals w.r.t. the input low frequency magnetic field.

Fig.7 shows the magnetic field measurements of the 3-axis magnetic sensor. Fig.7a shows the measurement setup of different magnetic field input directions. Measurement result shown in Fig.7b indicates the output voltage of the 3-axis magnetic sensor while varying the intensity of applied magnetic fields. The measurement results indicate the sensitivities of the magnetic sensor are respectively 7.72μV/mT for Y-axis, 18.86μV/mT for Z-axis, and 3.38μV/mT for X-axis respectively. The Z-axis sensitivity is higher due to its higher mechanical quality factor. The difference between the X-axis and Y-axis sensitivities is due to the discrepancy of the torsional stiffness and quality factor. Moreover, the measured noise floor in the spectra indicates the magnetic field resolutions of the presented sensor, which is 9.15uT/rtHz for Y-axis, 2.7uT/rtHz for Z-axis and 13.8uT/rtHz for X-axis respectively. Note that the readout circuit (an active probe) of this study has 0db gain. Thus, with the modification of the sensing circuitry and the system integration, the sensor performances can be further improved.

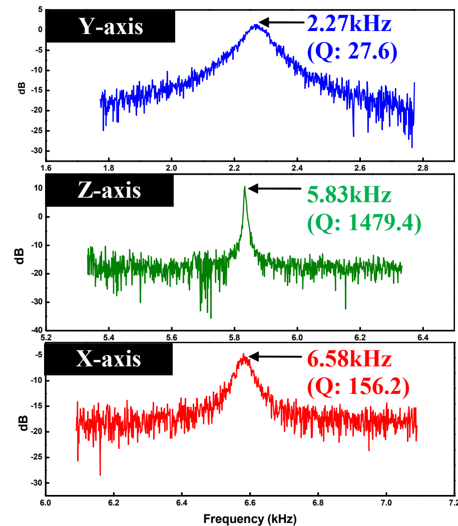

Figure 5: Measurement results of 3-axis sensing resonant frequencies.

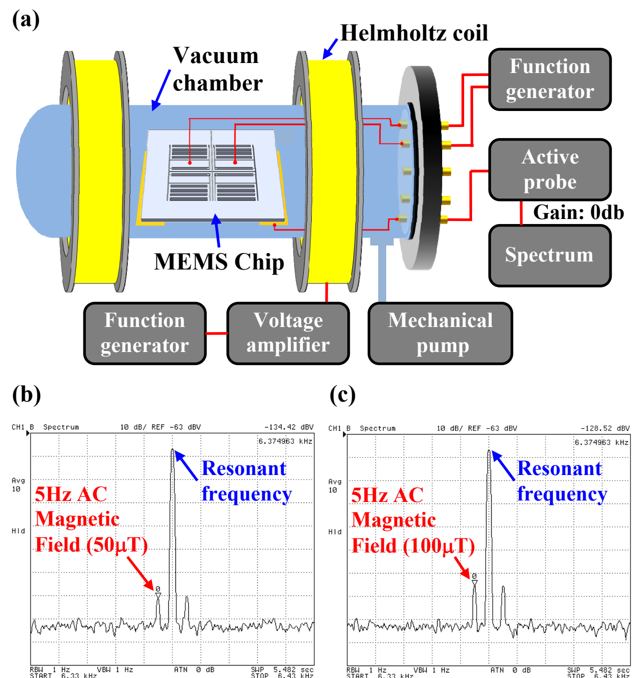

Figure 6: Measurement results of (a) measurement setup, (b) typical measured spectra in response to the X-axis magnetic field with intensity of 50μT, and (c) X-axis magnetic field with intensity of 100μT.

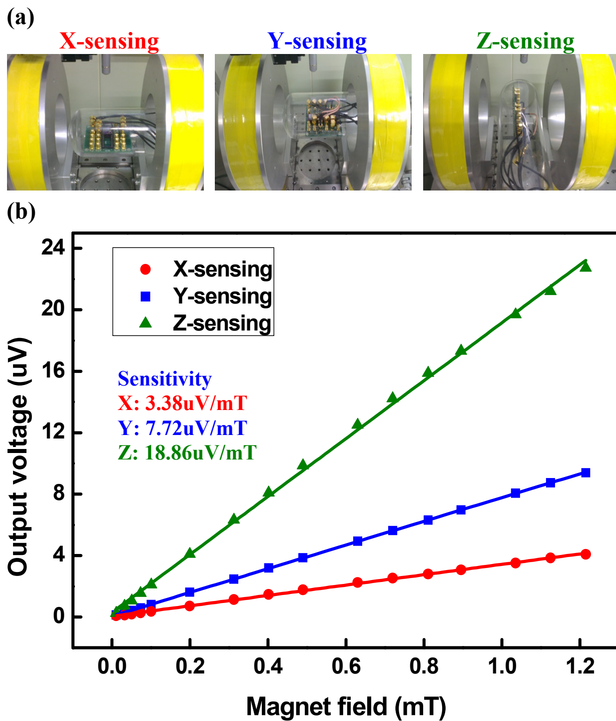

Figure 7: Measurement results of (a) different axes measurement setup, and (b) output voltages varying with intensity of three axes magnetic fields.

CONCLUSION

In this study, a silicon-based 3-axis Lorentz-force resonant-type magnetic sensor with single proof-mass has been proposed and implemented by the TSMC MEMS above CMOS process scheme. The Lorentz-force is induced by single current loop, and the torsional/in-plane translational motions are introduced to sense the 3-axis magnetic fields. Measurement results show the sensitivity of the magnetic sensor is 7.72μV/mT for Y-axis, 18.86μV/mT for Z-axis, and 3.38μV/mT for X-axis respectively. It can be improved by the circuitry modifications. Moreover, the resolution of this device is 9.15uT/rtHz for Y-axis, 2.7uT/rtHz for Z-axis and 13.8uT/rtHz for X-axis respectively. The process scheme is compatible with that for inertial sensors, thus, has the potential for future high-end applications, like IMU, IoTs products.

ACKNOWLEDGEMENTS

This paper was partially supported by the Ministry of Science and Technology of Taiwan (grant number MOST-104-2221-E-007-016-MY3), and National Applied Research Laboratories of Taiwan (grant number NARL-IOT-104-001). The authors would also like to appreciate the Taiwan Semiconductor Manufacturing Company Ltd (TSMC) for manufacturing service and Center for Nanotechnology, Materials Science and Microsystems (CNMM) of National Tsing Hua University and the National Nano Device Laboratory (NDL), Taiwan for the fabrication facility.

REFERENCES

[1] C. M Liu, C. S. Chou, C. F. Tsai, Y. M. Shen, S. F Chen et. al., "MEMS technology development and manufacturing in a CMOS foundry," *Transducers*, Beijing, June 5-9, pp.807-810, 2011.

[2] J. Lenz, and A. S. Edelstein. "Magnetic sensors and their applications," *Sensors Journal*, vol.6, pp.631-649, 2006.

[3] K. Skucha, P. Liu, M. Megens, J. Kim and B. Boser, "A compact Hall-effect sensor array for the detection and imaging of single magnetic beads in biomedical assays," *Transducers*, Beijing, June 5-9, pp.1833-1836, 2011.

[4] M. Suzuki, T. Fukutani, T. Hirata, S. Aoyagi, S. Shingubara et. al., "Triaxis magnetoresistive (MR) sensor using permalloy plate of distorting magnetic field," *IEEE MEMS,* Hong Kong, Jan. 24-28, pp.671-674, 2010.

[5] C. I. Chang, M. H. Tsai, C. M. Sun and W. Fang, "Development of CMOS-MEMS in-plane magnetic coils for application as a three-axis resonant magnetic sensor," *J. Micromech. Microeng.*, vol.24, pp.035016, 2014.

[6] M. Li, V. T. Rouf, M. J. Thompson and D. A. Horsley, "Three-axis Lorentz-force magnetic sensor for electronic compass applications," *J. Microelectromech. Syst.*, vol.21, pp.1002-1010, 2012.

[7] H. Emmerich and M. Schofthaler, "Magnetic field measurements with a novel surface micromachined magnetic-field sensor," *IEEE Trans. Electron Devices*, vol.47, pp.972-977, 2000.

[8] M. J. Thompson and D. A. Horsley, "Parametrically amplified z-axis Lorentz force magnetometer," *J. Microelectromech. Syst.*, vol.20, pp.702-710, 2011.

[9] C. W. Kung, F. Y. Lee, C. I. Chang, S. S. Li and W. Fang, "Sensitivity improvement of a resonant 3-axis magnetometer using dual mass vibrating system," *IEEE Sensors*, Valencia, Nov. 2-5, pp.714-717, 2014.

[10] M. Li, E. J. Ng, V. A. Hong, C. H. Ahn, Y. Yang et. al., "Single-structure 3-axis Lorentz force magnetometer with sub-30 nt/$\sqrt{}$hz resolution," *IEEE MEMS*, San Francisco,, Jan. 26-30, pp.80-83, 2014.

[11] C. W. Cheng, K. C. Liang, C. H. Chu, D. A. Horsley, and W. Fang, "Single chip process for sensors implementation, integration, and condition monitoring," *Transducers*, Barcelona, June 16-20, pp.730-733, 2013.

CONTACT

* W. Fang, tel: +886-3-5742923; fang@pme.nthu.edu.tw